

# Contents

<b>1</b>	<b>Electric characterization</b>	<b>3</b>
1.1	Electric scheme and description . . . . .	3
1.2	Output characterization . . . . .	5
1.2.1	Measures without gas . . . . .	5
1.2.2	Measures with gas . . . . .	7
1.2.3	Time intervals . . . . .	8
1.2.4	Effective current . . . . .	8



# Chapter 1

## Electric characterization

### 1.1 Electric scheme and description

Development of electric scheme used to build Plasma Coagulation Controller is highly influenced by the need of flexibility in output and mobility for wound treatment. To produce plasma as DBD, in air with Helium or Argon as ignition gasses, it is necessary to apply high electric fields in little space, while to permit easy medical application the design of the head must be compact with particular attention to electric safety measurements. It is common to produce electric fields with fast voltage pulses for various uses, including jet or DBD plasma production ([9], [3], [2]), the scheme used in this study outputs a voltage pulse with an amplitude up to 10 kV and frequencies up to 60 kHz.

A representation of power and signal lines is in figure 1.1. The circuit is divided mainly in two parts : the controller, with alimentation and settings controls, and the head, where the discharge happens and plasma is emitted.

The line divides in:

- **Alimentation** : the 220 V DC power line goes in a transformer that gives a 22 V tension to the head, passing through a diode bridge. This tension alimnts the Driver Circuit on the head.
- **Arduino and trigger** : the power line is reduced to 12 V necessities to aliment an Arduino controller and a laser. From an analogical output of the Arduino a PWM wave goes to the laser trigger, it transmits information on the wave, frequency and duration, with an optical fiber that ends with a photodiode installed on the driver circuit. Wave frequency is setted by the Arduino, wave duration is setted giving the opening time of the MOSFET that passes the signal to be amplified and sent to the head's transformer. With this setup the high-voltage line is entirely decopuled from the controller, so there are not problems of signal reflection on the power line or the Arduino.
- **Head** : the Driver Circuit receives a power line of 22 V and an optical trigger that defines frequency and duration of the voltage pulse. When the trigger gives the start

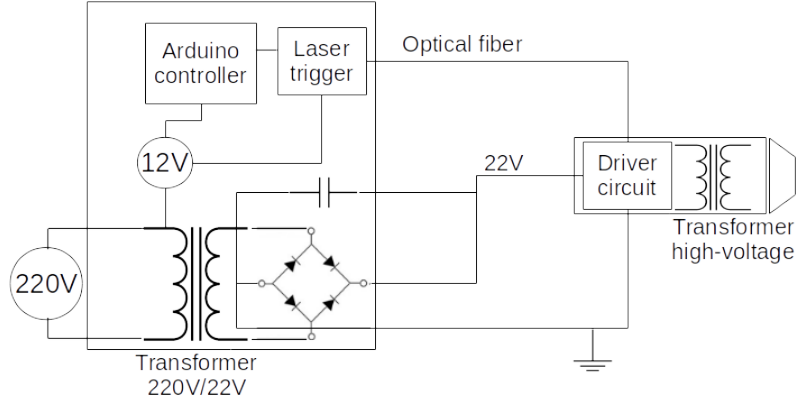


**Figure 1.1:** Scheme of the general electric line to produce high voltage, the controller on the left and the head on the right.

signal, the transformer on the head receives on primary circuit a voltage of hundreds V and outputs from secondary circuit a voltage of thousands V. Connected to the output there is the electrode inside a capillary tube of dielectric material.

To understand signal propagation is presented a simulation in figure 1.2, obtained with a simplified scheme with Spice. As shown, once the PWM trigger starts, tension on the primary goes from alimentation value to 0, when the PWM signal ends (after  $6\mu\text{s}$ , it has a pulse with amplitude of 150 V (width of  $1.2\mu\text{s}$ ) and a pulse of  $-5000\text{ V}$  at the output of secondary circuit. A longer PWM implies a longer charging time, so an higher pulse. Ultimately, amplitude of the pulse is proportional to the width of the PWM signal and to know working conditions of the source it is necessary to study the relation between opening time and amplitude output on the actual circuit.

During this thesis study were built two sources, with two controllers and heads, the first one will be called source A, the second one source B. From an electrical perspective the two models are almost identical, the second one comes with a low-pass filter on the driver circuit (to diminish high frequencies noise) and higher amplitude capabilities thanks to a different turns ratio of head's transformer. The characterization of electric features is made measuring output tension and current with different settings for the pulse.

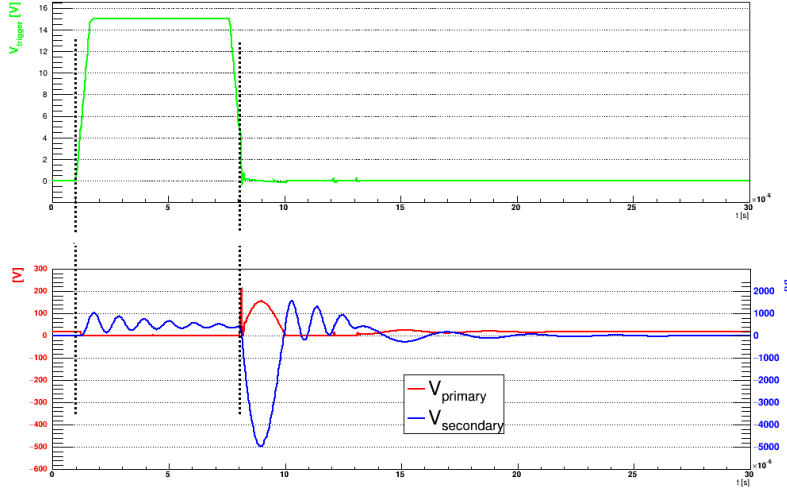


**Figure 1.2:** Scheme of signal propagation. Up, in green, there is the optical trigger, down, in red, the voltage of primary circuit in the head with axis on the left, in blue, the voltage of secondary circuit with axis on right.

## 1.2 Output characterization

Plasma ignition and discharge features are regulated by electric field generated in the circuit head and power deposition to flowing gas, so the parameters involved are pulse amplitude and frequency arriving on the electrode, settable in the circuit. Medical application of plasma requires low current intensity, in this study it's measured the current flowing on a copper plate targeted by the plasma plume at a certain distance. Ultimately the different parameters for the measures are:  $\Delta t$ , opening time of the trigger that defines amplitude of the pulses, and  $f$ , frequency of the pulses.

Voltage signal are taken with an high-voltage probe, attenuation  $\times 1000$ , current signal with a *Tektronix CT2* probe that gives a 1 mV for a current of 1 mA. All signals are measured with a *Yokogawa DL9040* oscilloscope, from which is saved the waveform of voltage and current.

Measures are taken without gas flowing, to see the output voltage of the circuit, and with an helium flow of 2 L/min, to measure the actual output with different amplitude and frequencies. It's also measured an effective current intensity, i.e. a mean value in a time period, to evaluate plasma application's effects on biological tissues.

### 1.2.1 Measures without gas

It's used the hv probe to pick tension difference between secondary circuit output and ground. Once a work frequency,  $f$ , is set, we take voltage wave shape for different values of opening time of the circuit,  $\Delta t$ , in the selectable range. To assure that a voltage pulse ends before another starts, this range is different for different frequencies: higher work frequencies means more pulses in a given time, taking into consideration pulse oscillations

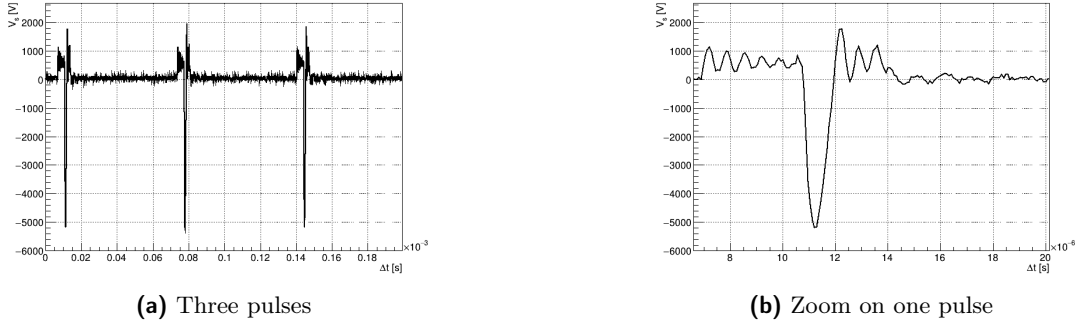


**Figure 1.3:** Example pulses with source B for  $f = 10$  kHz and  $\Delta t = 2$   $\mu$ s

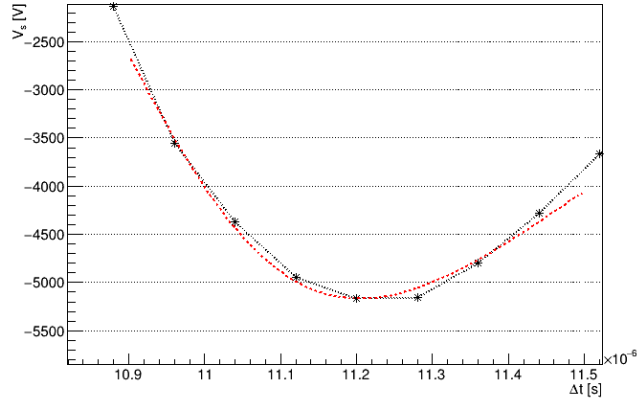
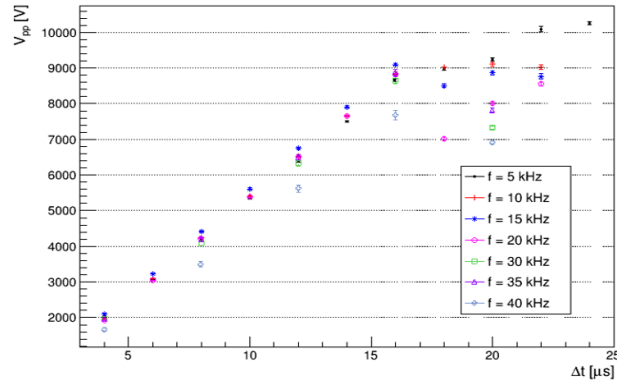


**Figure 1.4:** Example fit with source B for  $f = 10$  kHz and  $\Delta t = 2$   $\mu$ s

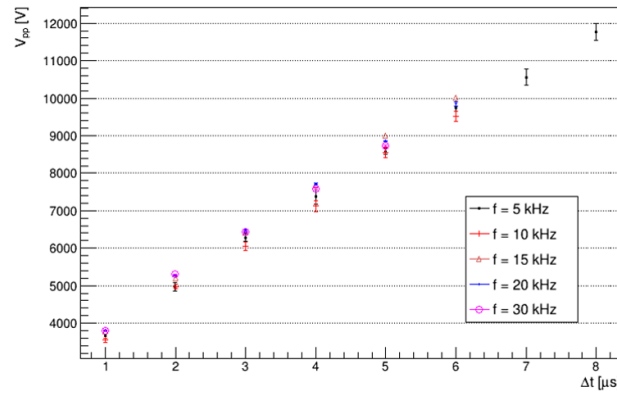
time width, proportional to opening time, the range of possible  $\Delta t$  is smaller at higher frequencies. A typical obtained measure is shown in figure 1.3.

The main purpose of the measures is to study proportionality between amplitude of the peak and opening time, for different frequencies. Those signals are analyzed evaluating their Fourier Transform (using ROOT C++ libraries [6]) and reconstructing the signal without higher frequencies, to exclude noise fluctuations. The reconstructed peak is an asymmetric function as in figure 1.4, it's possible to interpolate it with a Landau function [1] and obtain peak value and position. The error from the fit function is added quadratically to the error given by the cut of high Fourier frequencies, evaluated as the square root of the mean square error between reconstructed and original signal for every point included in the fit range.

Results are shown in figure 1.5 for the two sources. In source A we can see a linear behavior for  $4 \leq \Delta t \leq 16$   $\mu$ s, with tensions from 2 to 9 kV; for greater  $\Delta t$  data loses linearity. The upper limit on chosen  $\Delta t$  is given by the need of a minimum time interval between two pulses. Also in source B we can see a linear behavior, but tensions are much



(a) Source A



(b) Source B

**Figure 1.5:** Absolute peak's value of secondary circuit in function of  $\Delta t$  at different  $f$ , for both sources.

larger: for  $1 \leq \Delta t \leq 8 \mu s$  tension goes from 4 to 12 kV. With this source the upper limit for  $\Delta t$  is given by voltage output, measures are taken only for tensions needed to have plasma in a DBD regimen, higher opening times would only stress more circuit components. Both sources have near the same output for different frequencies, to confirm it data are fitted with a linear function in the range  $0 - 16 \mu s$  for source A and range  $0 - 8 \mu s$  for B. Evaluated parameters are compared, as shown in figure 1.6. The values are displaced with random distances from the mean value, so it can be concluded that the behavior is not defined by the frequency.

### 1.2.2 Measures with gas

Introduction of an helium flow at the end of the head will produce plasma ignition, tension will be different, and it will be possible to measure intensity of the current carried by

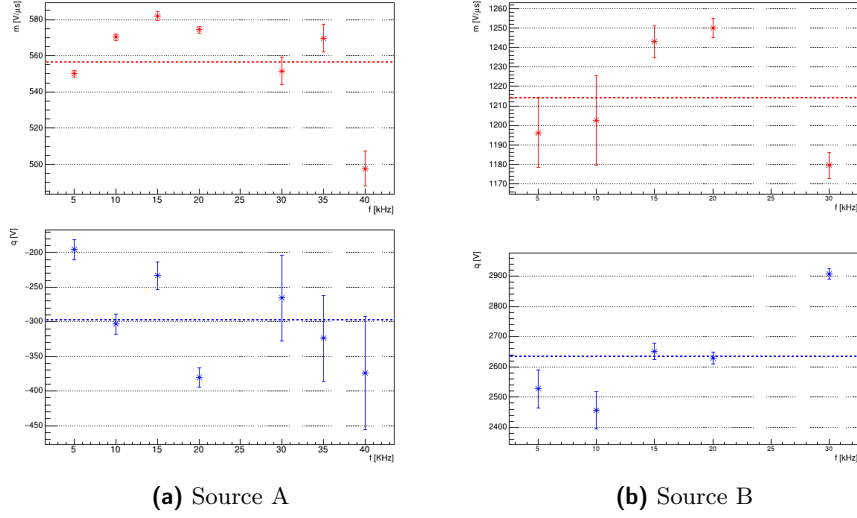


**Figure 1.6:** Linear fit parameters of  $V_{peak}(\Delta t)$  for both sources.

plasma. To assure safety of plasma application, that cells aren't damaged by plasma, it must be avoided a large current intensity and arc formation. Studies of conditions for DBD discharges and arc transitions ([4], [7], [8]) suggests that maximum current values are in the order of hundreds of mA.

Current intensity is measured using a copper sheet with dimensions  $1\text{ cm} \times 1\text{ cm} \times 0.1\text{ cm}$ . Plasma plume impacts on the sheet, the current probe is connected to it and send the signal to the oscilloscope, with cable shielding to lessen interferences. Distance from source head and target is chosen with a typical value for treatments, relation between current and target distance is studied in [5].

In figure ?? can be seen a typical measure for  $\Delta t =$  and  $f =$  with source A.

### 1.2.3 Time intervals

### 1.2.4 Effective current



# Bibliography

- [1] R. Brun. *ROOT documentation for Landau() function*. 1995. URL: <https://root.cern.ch/doc/master/namespaceTMath.html#a656690875991a17d35e8a514f37f35d9>.
- [2] T Darny et al. “Analysis of conductive target influence in plasma jet experiments through helium metastable and electric field measurements”. In: *Plasma Sources Science and Technology* 26.4 (2017), p. 045008. DOI: 10.1088/1361-6595/aa5b15. URL: <https://doi.org/10.1088/1361-6595/aa5b15>.
- [3] Julien Jarrige, Mounir Laroussi, and Erdinc Karakas. “Formation and dynamics of plasma bullets in a non-thermal plasma jet: influence of the high-voltage parameters on the plume characteristics”. In: *Plasma Sources Science and Technology* 19.6 (2010), p. 065005. DOI: 10.1088/0963-0252/19/6/065005. URL: <https://doi.org/10.1088/0963-0252/19/6/065005>.
- [4] U. Kogelschatz, B. Eliasson, and W. Egli. “Dielectric-Barrier Discharges. Principle and Applications”. In: *Journal de Physique IV Colloque* 07.C4 (1997), pp. C4–47–C4–66. DOI: 10.1051/jp4:1997405. URL: <https://hal.archives-ouvertes.fr/jpa-00255561>.
- [5] Cecilia Piferi. “Caratterizzazione di sorgenti di plasma per applicazioni biomediche”. 2016/17.
- [6] *ROOT documentation for TVirtualFFT class*. URL: <https://root.cern.ch/doc/master/classTVirtualFFT.html>.
- [7] Takaaki Tomai, Tsuyohito Ito, and Kazuo Terashima. “Generation of dielectric barrier discharge in high-pressure N2 and CO2 environments up to supercritical conditions”. In: *Thin Solid Films* 506-507 (2006). The Joint Meeting of 7th APCPST (Asia Pacific Conference on Plasma Science and Technology) and 17th SPSM (Symposium on Plasma Science for Materials), pp. 409–413. ISSN: 0040-6090. DOI: <https://doi.org/10.1016/j.tsf.2005.08.101>. URL: <http://www.sciencedirect.com/science/article/pii/S0040609005013052>.
- [8] Lewi Tonks and Irving Langmuir. “A General Theory of the Plasma of an Arc”. In: *Phys. Rev.* 34 (6 1929), pp. 876–922. DOI: 10.1103/PhysRev.34.876. URL: <https://link.aps.org/doi/10.1103/PhysRev.34.876>.

- [9] J. Upadhyay et al. “Development of high-voltage pulse generator with variable amplitude and duration”. In: *Review of Scientific Instruments* 85.6 (2014), p. 064704. DOI: 10.1063/1.4884883.